Journal of Materials Chemistry A

Accepted Manuscript

ROYAL SOCIETY OF CHEMISTRY

www.rsc.org/materialsA

Galactomannan binding agents for silicon anodes in Li-ion batteries

Martin K. Dufficy, Saad A. Khan, Peter S. Fedkiw*

Department of Chemical and Biomolecular Engineering, North Carolina State University, Raleigh, NC 27695

Email: fedkiw@ncsu.edu

Keywords: Silicon anode, Galactomannan, Silicon binder, lithium-ion battery, polysaccharide

Abstract

The challenge to incorporate Si into Li-ion battery anodes has attracted much attention. Binding agents are a critical component in a battery that may also be used to enhance electrode performance. Herein, we report the use of galactomannans—a low-cost, environmentally friendly, biorenewable polymer—as a novel binding agent for Si-containing electrodes. Silicon-containing electrodes with as low as 5 wt% binder show large reversible capacities with > 90% charge retention after 100 cycles without the use of electrolyte additives. Large capacities and low binder content when compared to carboxymethyl cellulose allows for greater energy densities and fast Li-extraction for high-power applications. The performance enhancement may be attributed to polymer-particle interactions between the hydroxyl groups of galactomannans and native-oxide layer of Si. These interactions, coupled with the inherent mechanical integrity of galactomannan thin films, allow for minimal cracking and delamination of the electrode upon lithiation. An undamaged electrode microstructure during large volume expansions allows for coulombic efficiencies > 99%. Galactomannans also experience ample polymer swelling in common electrolyte solvents, which leads to rapid Li transport and higher ionic conductivities than other biopolymer-bound electrodes. Galactomannan binders may thus provide a critical step forward in next-generation lithium-ion batteries.

Introduction.

Lithium-ion batteries (LIBs) are a ubiquitous power source for portable electronic devices. The appeal for LIBs manifests in an energy and power density exceeding >200 Wh kg^{-1} and 300 W kg^{-1}, respectively[1]. However, improvements are imperative for electric vehicle applications[2]. A decrease in cost and an increase in energy density are needed before electric vehicles can compete competitively in the market with internal combustion engine vehicles. Research is looking into cheaper materials and facile production procedures to drive costs lower. Many methods to increase energy density focus on implementing high-capacity materials such as silicon in LIB anodes[3,4]. Silicon has a theoretical charge capacity of 4.2 Ah g^{-1} but suffers from pulverization and electronic isolation upon prolonged cycling. The pulverization stems from the large (>300%) volume expansions upon lithiation that lead to cell failure. Researchers have employed three disparate approaches to prolong the cycle life of Si-based electrodes: 1) varying electrode architecture[5], 2) composite carbon/Si materials[6–8], and 3) electrode binding agents[9–13]. The first two methods require rigorous multi-step processing conditions that increase cost, leading to increased attention in exploring novel binding materials. Some binders currently used in electrode materials pose a health risk, as the casting processes require harsh solvents, for example, N-methyl-2-pyrrolidone (NMP) is commonly used to prepare the binder polyvinylidene fluoride (PVDF). The need to implement environmentally benign and abundant binding materials that function at low loadings is an issue facing lithium-ion battery technology. One potential class of binding materials for LIBs are galactomannans.

Galactomannans are polysaccharides found in leguminous seed endosperm and account for the majority of seed content. The biopolymers have many commercial applications including usage in the food, textile, and petroleum industries[14–16]. Two galactomannan biopolymers, guar gum (GG) and locust bean gum (LBG), are shown in **Figure 1**. The difference in molecular composition of galactomannans lies in the degree of substitution, or the amount of galactose side-chains distributed throughout the mannose backbone. Guar gum has a mannose (M) to galactose (G) concentration (M:G) of ~2:1, whereas LBG has

that of ~4:1. The degree of substitution gives each galactomannan unique properties such as viscosity, strength, and biopolymer self-association[17,18].

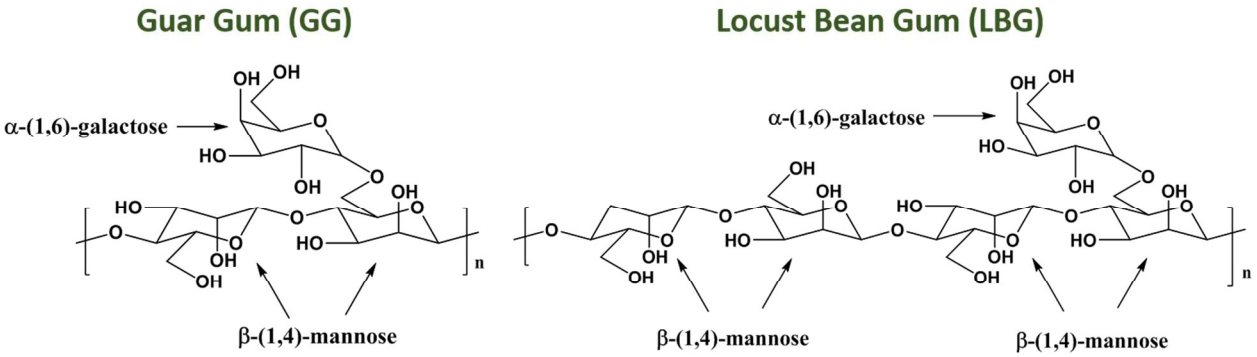

Figure 1. The chemical composition of guar gum (GG) and locust bean gum (LBG). Galactomannans are polysaccharides comprised of a mannose backbone and galactose side-chains, which can be distributed randomly or in blocks[19] throughout the molecule.

Herein, we report that galactomannans may be used as an environmentally friendly binding agent for Si electrodes. Galactomannan binders have recently been employed in Li-titanate electrodes[20], here we report use of galactomannan binders in Si-containing electrodes of much lower potential and significant volume change upon Li insertion/extraction. The novelty of this work lies in the low-binder content of galactomannans used to obtain high charge capacities. Unlike other polysaccharide binders for Si anodes[13,21] that require up to 25 wt.% binder and an excess of conductive additives, we observe large capacities and prolonged electrode stability at much lower galactomannan-binder loadings (5 wt%), decreasing the amount of conductive carbon necessary and further increasing the electrode energy density. Electrode slurries are film-cast in an aqueous medium using a process similar to commercial coating methods. Galactomannan binders provide high Si-binding strength at low-binder concentrations in Li-ion anodes. The favorable particle-binder interaction and inherent mechanical strength of galactomannans allows for stable Li-ion performances with 90% discharge capacity retention upon 100 charge/discharge cycles with coulombic efficiencies (CEs) in excess of 99% after 250 cycles at 1-C charge/discharge rates; solid-electrolyte interface (SEI) stability is observed in the absence of electrolyte additives such as fluoroethylene carbonate (FEC). The results reported in this study using galactomannans

as binders provide a promising inexpensive alternative to carboxymethyl cellulose (Na-CMC) and PVDF binders.

Experimental

Materials

The binding materials used in the study are guar gum (GG, Sigma Aldrich), locust bean gum (LBG, Sigma Aldrich), carboxymethyl cellulose sodium salt (Na-CMC, Sigma Aldrich), and Kynar 500 polyvinylidene fluoride (PVDF, Arkema). The conductive carbon Super P Li (Timcal Graphite & Carbon) and silicon nanoparticles (SiNPs, Alfa Aesar, average particle size ≤ 50 nm) complete the balance of electrode materials. Guar gum, LBG, and Na-CMC were dissolved in DI water (18.2 MΩ-cm, Millipore) while PVDF was dissolved in anhydrous N-methyl-2-pyrrolidone (NMP, 99.5% purity, Sigma Aldrich). The slurries of SiNPs + carbon + binder were cast onto copper foil (9-µm, MTI Corporation) and cycled against a Li counter/reference electrode (Sigma Aldrich) in a coin cell (2032, MTI Corporation). A separator (Celgard, 25-µm thick) prohibited physical contact between the electrodes. Electrodes were wetted with an ethylene carbonate (EC, 99% pure, Sigma Aldrich) + ethyl methyl carbonate (EMC, Ferro Corp.) mixture with lithium hexafluorophosphate salt ($LiPF_6$, BASF). The electrolyte solvents were dried in molecular sieves (4A, Sigma Aldrich) to a water content < 10 ppm. Anhydrous acetonitrile (Acros Organic) was used to wash cycled electrodes.

Binder purification and dissolution

The biopolymers Na-CMC, LBG, and GG were purified for 7 days in dialysis tubing (14 kDa MW cutoff) to remove low-molecular weight impurities. After dialysis, the biopolymers were dried in a vacuum oven at 40°C. A LBG solution in water was heated and stirred at 80°C for at least 24 hrs to fully dissolve the polymer. The solution was cooled to room temperature before casting a film. Guar gum and Na-CMC were dissolved in water while PVDF was dissolved in NMP, all at room temperature. This study addressed the effect of various binder loadings in SiNP electrodes. Polymer solution concentrations were

varied to prevent the aggregation of hydrophobic carbon in the aqueous slurry and to adjust dispersion viscosity to enable coating, for example, casting SiNP electrodes using LBG binders (SiNP/LBG) required 0.7-1 wt%, while polymer with lower viscosities such as Na-CMC required concentrations of 2-3 wt%.

Half-cell fabrication

Si-based electrodes comprising 75, 80, or 85 wt% SiNPs + 10 wt% C + balance binder solution, were placed into a mortar. A pestle was used to mix the materials for at least 20 minutes. Films cast onto Cu foil (0.75 mg cm^2 SiNP loading, ~11.3 mg total disk weight) were placed in a convection oven at 80°C for 30 mins to dry. Disks of 1.27-cm diameter were punched from the coated Cu foil and placed in a vacuum oven at 120°C for at least 18 hours. The dried disks were transferred to an argon-filled glove box and placed into button half-cells with polished lithium as the counter and reference electrode. The electrolyte, 1 M $LiPF_6$ in 1:1 wt EC: EMC, was added by pipette onto the working electrode (~50 µL) and the Celgard separator (~50 µL). The half-cell can was hermetically crimped with a stainless steel spacer and spring on top of the Li metal to guarantee good contact. Polymer-only films for cyclic voltammetry and impedance testing were made by casting a polymer solution on Cu foil with the doctor-blade gap height set to 1 µm. The drying and assembly process was identical to the aforementioned Si-based electrodes. A 24-hour rest period was given to all half-cells after fabrication to stabilize open-circuit potential.

Electrochemical testing

A capacity of 3600 mAh g^{-1} was used to calculate C-rates for electrochemical experiments. Unless otherwise stated, cells were cycled between 1 V and 10 mV vs. Li/Li^+ using an Arbin BT2000 battery cycler. Cyclic voltammetry was performed with a Princeton Analytical Research VersaSTAT 4 potentiostat between 3.4 V and -25 mV vs Li/Li^+ for polymer-only films, and between 1V and 10 mV Li/Li^+ for SiNP electrodes. Electrochemical impedance spectroscopy (EIS) was conducted on polymer films using a VersaSTAT 4 with frequencies between 100 MHz and 10 mHz and amplitude of 10 mV.

Impedance was measured at 10 mV vs Li/Li^+. Prior to EIS measurements, the cells were held at 10 mV for at least 6 hrs. At least 4 half-cells were used for all electrochemical tests to assess reproducibility of the results. All measurements were performed at ambient conditions.

Solvent Uptake

Polymer films were produced by casting equal amounts of 2 wt% polymer solutions into Teflon molds and drying at ambient temperatures. Once dry, the films were removed from the molds and placed in a vacuum oven at 120°C overnight to remove solvent. The films were immediately transferred to a glove box, weighed, and placed into electrolyte (1 M $LiPF_6$ in 1:1 wt EC: EMC). After 24, 48, and 72 hours, the films were carefully blotted dry to remove excess surface electrolyte and weighed.

Physical Characterization

Infrared spectroscopy was used to determine the presence of functional groups on SiNPs, the binder, and the electrodes using a Thermo Scientific Nicolet 6700 FT-IR. The crystallinity of the SiNPs was observed by X-Ray Diffraction (XRD) on a Rigaku SmartLab X-ray diffractometer (Cu K_α, λ = 1.54060 Å). The size of the crystallites was calculated using the Scherrer equation and averaging the particle size for the (111), (220), and (311) peaks. All SEM images were captured on an FEI XHR Verios 460L. Low operating voltages ($\leq$ 1 kV) and a stage bias (700 V) were used to prevent sample charging. Conductive coatings were not applied to better observe surface structure and morphology. To image the electrodes post-mortem, the button cells were first decrimped and washed in acetonitrile to remove the electrolyte. This process was conducted in a glove box. The electrodes were removed and transferred to a vacuum oven and dried at 120°C overnight. Steady shear viscosity of polymeric binder solutions were measured using a stress-controlled rheometer (Discovery Hybrid Rheometer-2, TA Instruments). A 4-cm cone with a 2° geometry was used for all experiments.

Results and Discussion

This study examines two types of galactomannans for their use as binding agents for Si-based electrodes in LIB anodes, guar gum (GG) and locust bean gum (LBG). Many researchers have observed interactions between SiNPs and other polymers used for binders such as alginate[11], carboxymethyl cellulose[22] (Na-CMC), and polyacrylic acid[23] (PAA). All are polyelectrolytes that contain carboxylic groups capable of H-bonding or undergoing a condensation reaction with the native-oxide layer of SiNPs[17]. The strong Si-binder interactions are thought to play a major role in electrode stability[11,22,23]. Galactomannans do not contain carboxylic groups, and we hypothesize that H-bonding interactions occur between the less polar –OH groups (mainly from galactose) and the oxide layer of SiNPs to promote electrode stability during charge/discharge cycling. The FT-IR spectra (**Figure 2a**) of SiNPs, GG, and cast SiNPs electrodes using a GG binder (SiNP/GG) provide evidence for H-bonding interactions. Many peaks in the GG spectrum arise from the polymer backbone, including sp^3 stretching and bending at ~2920 and ~1390 cm^{-1}, respectively, and C-O-C antisymetric vibrations at ~1150 cm^{-1}. However, of importance for H-bonding is the peak at ~3420 cm^{-1} corresponding to –OH stretching, which is present in all three sample spectra, and the peaks between 1150 and 1000 cm^{-1} corresponding to secondary alcohols in GG[14]. The SiNP spectrum displays peaks between 900-1200 cm^{-1} that correspond to Si-O-Si bonding and confirm the presence of a native-oxide layer. Additional peaks corresponding to Si-OH[24] and Si-H[25] stretching at ~3650 and 2110-2140 cm^{-1}, respectively, suggest a functionalized surface capable of H-bonding with galactomannans.

Studies[26] suggest that galactomannans with a low degree of substitution (high M:G) undergo self-association; the mannan regions preferentially bind with other mannan regions[27,28] giving LBG a higher solution viscosity (**Supplemental Figure S1**) and lower solubility in water than more-substituted galactomannans. Although the solution viscosities of galactomannans are high (30 Pa·s at 2 wt% LBG) and the solutions cannot be cast using a doctor-blade method, the galactomannans undergo syneresis as a

result of the milling process. The solvent extraction that occurs allows for slippage in the casting method, and uniform films are produced. Regardless of mannose concentration, the high viscosity of galactomannan solutions arises from the hydrogen bonding (H-bonding) of the –OH groups and facilitates production of homogenous electrode materials without particle settling. Harding's group proposed[29] that the mannose and galactose monomer contribute to the hydrophobic and hydrophilic nature of the galactomannan, respectively. Thus, the more hydrophilic galactose regions would preferentially bind to the native-oxide layer of SiNPs. A cartoon of the proposed SiNP-galactomannan interactions (**Figure 2b**) depicts: 1) H-bonding, preferentially between the galactose side groups and the oxide layer of SiNPs, and 2) self-association between the mannan backbone, which may reduce the amount of mobile galactose sites.

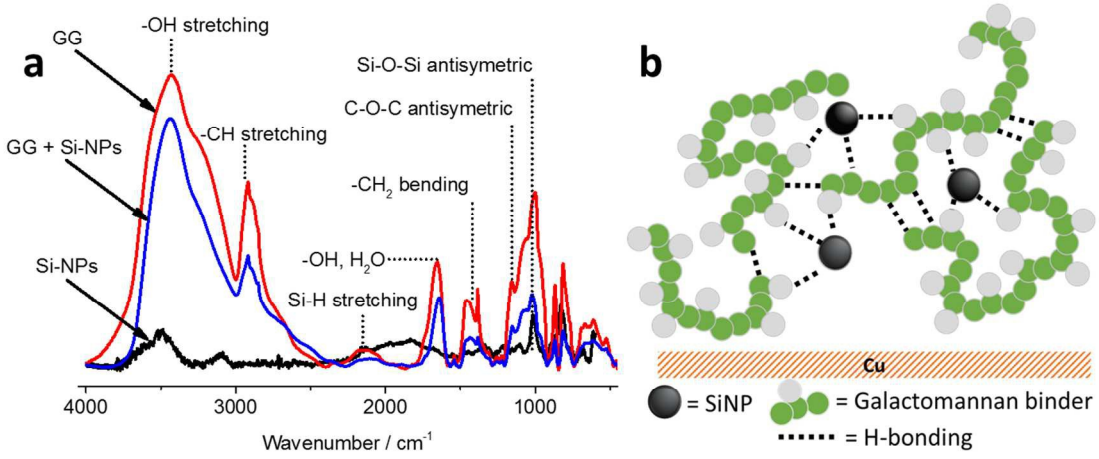

Figure 2. a) FT-IR spectra of GG, SiNPs, and the composite electrodes. Hydroxyl groups are observed on the surface of both GG and SiNPs; b) Depiction of H-bonding that may contribute to the good cyclability of electrodes using GG binders. The grey circles correspond to the galactose side-groups on the GG backbone.

Prior to electrochemical cycling, the electrodes contain crystalline SiNPs, as determined via XRD (**Supplemental Figure S2**) with an average crystallite size of 42 nm, which is different than the average particle size of 58 nm observed via HR-SEM imaging. A bimodal particle-size distribution, an artifact of SiNP processing[30], is observed from the HR-SEM images and is one potential cause for the size disagreement between XRD and SEM measurements (**Supplemental Figure S2**). Composite SiNP

electrodes with 5 wt% GG + 10 wt% C + 85 wt% SiNP (**Figure 3 a, b**) result in a void volume of ~30%, as determined via ImageJ software (National Institutes of Health). Images with binder loadings of 10 and 15 wt% for both GG and LBG (**Supplemental Figure S3**) reveal a nanostructure and porosity similar to the electrodes cast with 5 wt% binder; a higher-binder content did not fill voids in the electrode structure. The porosity of the film allows for electrolyte infusion, rapid Li-ion transport and accommodates electrode expansion during lithiation.

After 50 charge/discharge cycles in a half-cell at a 1-C rate (3.6 A g^{-1}) between 1 V and 10 mV vs. Li/Li^{+}, SEM images of the SiNP/GG electrodes (**Figure 3 c, d**) reveal a resilient porous nanostructure after deep-lithiation cycling. The SiNP/GG electrodes retain the pre-cycling microstructure and the active materials remain in electronic contact to allow for rapid (de)lithiation. The presumed thinness of the GG coating, consequence of the low-binder loading, leads to a mechanically durable electrode that limits pulverization during volume expansions exceeding 300**%.** Macro-scale electrode cracking, a common feature found in SEM post-mortem analysis of Si-based electrodes, is attributed to a loss in electrode activity[31]. Significantly, we did not observe micro-scale cracking in the images of SiNP electrodes using galactomannan binder. In contrast, images of SiNP electrodes using Na-CMC (SiNP/CMC) and PVDF (SiNP/PVDF) binders (**Supplemental Figure S4**) cycled through identical conditions do not retain their pre-cycling nanostructure, as much of the initial porosity is lost. Electrode cracking is a common observation in SiNP/CMC electrodes.

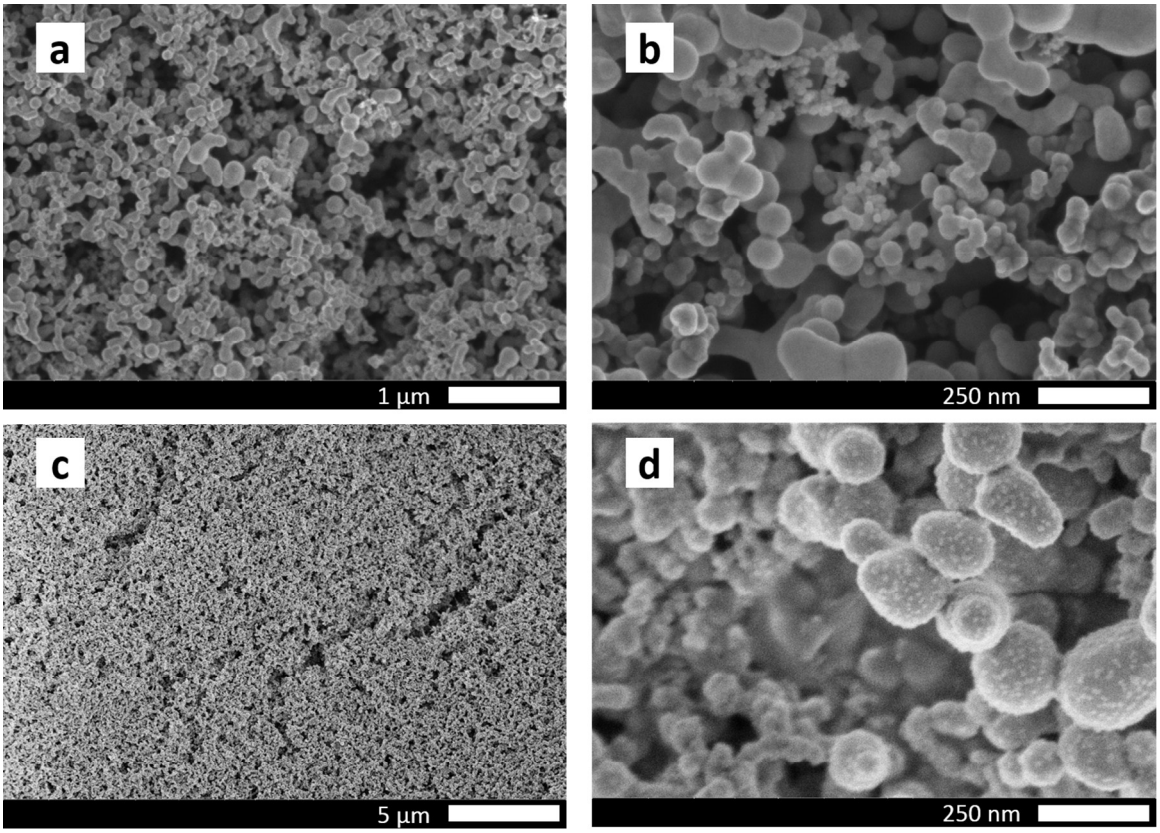

Figure 3. SEM images of (a, b) pre-cycled SiNP/GG electrodes and (c, d) post-cycled delithiated SiNP/GG electrodes. The porous structure is maintained after 50 cycles. The size of the SiNPs increase after cycling. Electrode composition is 85:10:5, SiNPs:C:Binder wt%.

Electrolyte uptake in the polymers provides insight on polymer-solvent interactions. Some degree of swelling is necessary in the binder to facilitate Li-transport through the polymer. The polymers investigated achieved a steady-state electrolyte uptake after 24 hours. Polymer-only films comprised of PVDF, LBG, GG, and Na-CMC submerged in electrolyte increase 39, 20, 14, and 6% in mass, respectively (**Figure 4a)**. The greater electrolyte uptake of galactomannan binders compared to Na-CMC may improve the rate performance of Si electrodes, as more Li-ions are able to insert/extract. The swelling of the films may also reduce brittleness in the polymer, reducing fractures upon lithiation. The small amount of electrolyte uptake in Na-CMC films and ensuing brittleness is postulated to be one reason for the electrode cracks observed in SiNP/CMC post-mortem analysis.

Li-ions travel through absorbed electrolyte in the polymer binder to reach Li-active host materials, and electrolyte uptake may consequently correlate with Li-ion conductivity. The ionic resistivity of a material may be gauged by fitting the high-frequency impedance data to an equivalent circuit and extrapolating the data to the x-intercept of a Nyquist plot. The impedance spectra (**Figure 4b**) of electrolyte-swelled LBG, GG, Na-CMC, and PVDF polymer-only films were fit to a Randles circuit. Resistances associated with the high-frequency resistor in the Randles circuit, including the solution and electronic contact, are considered constant; the variation in high-frequency resistor values stems from the ionic conductivity through the polymer film. A fit of the data reveals high-frequency resistor values of 12.7, 13.1, 16, and 9.1 ohms for GG, LBG, Na-CMC and PVDF films, respectively (**Figure 4b inset**). As expected, PVDF films with the most electrolyte solvent uptake yield the lowest high-frequency resistor values (least ionic resistance) while Na-CMC films with the least electrolyte solvent uptake have the highest high-frequency resistor values (most ionic resistance). There is an insignificant difference in the ionic resistance of galactomannan films based on the high-frequency impedance data. The galactomannan films have lower ionic resistances than Na-CMC films, which may facilitate the transfer of Li-ions through SiNP electrodes using galactomannans as binders. Because the films are not electrochemically active, the resistances remain constant between 0.01-3.5 V vs. Li/Li^+. Voltammograms on GG, LBG, Na-CMC, and PVDF (**Supplemental Figure S5**) also reveal the polymer-only films to be electrochemically inert over the same potential range, which suggests galactomannans may also be used as binders for cathode materials, although not explained in the present study.

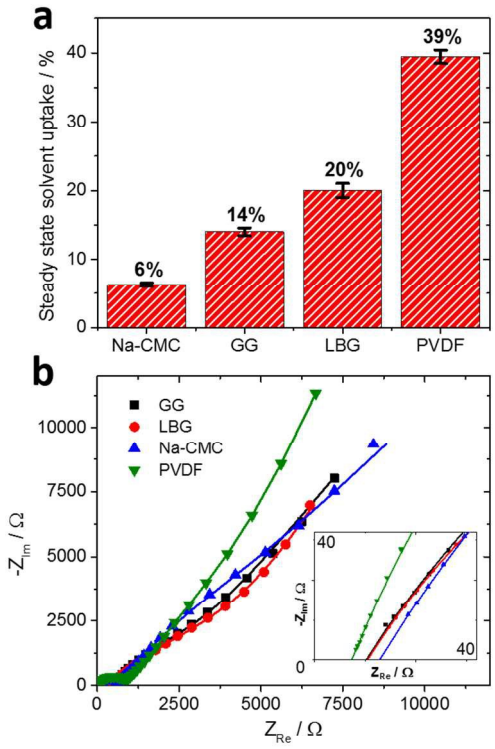

Figure 4. (a) Steady-state swelling of polymer-only films in 1 M $LiPF_6$ salt with EC:EMC (1:1 wt) solvents shows PVDF and galactomannans uptake more electrolyte than Na-CMC; (b) The EIS spectra of electrolyte-swelled PVDF, Na-CMC, LBG, and GG films deposited on Cu foil in the absence of Si and C show resistances that can be attributed to the binder material. The symbols represent the measured data and the lines correspond to an equivalent-circuit model. The inset shows the high-frequency data. EIS measurements were conducted at 10 mV vs Li/Li^+.

The lithiation of SiNPs at a 10 mV cutoff voltage may be used to gauge material properties of the polymer binders including the mechanical integrity of the binder during volume changes and at full lithiation, as well as the ability of the binder to adhere to the SiNPs via particle-polymer interactions. The SiNP electrodes using GG and LBG binders exhibited a delithiation capacity of 2150 and 1850 mAh g^{-1}, respectively, after 20 cycles at 0.05-C (**Figure 5**) while retaining 75% of the initial delithiation capacity. The higher capacity observed in SiNPs/GG electrodes when compared to SiNP/LBG may be attributed to an increase in the hydrophilic galactose groups bonding to the native-oxide layer of the SiNPs, which results in a more robust composite electrode. Because LBG films take in more electrolyte than GG films, we also hypothesize that electrolyte uptake may diminish particle-polymer interactions—galactose interactions in particular. Additionally, constant-current, constant-voltage cycling[32] of SiNP/GG and

SiNP/LBG electrodes using a 100 mV cutoff voltage produce stable delithiation capacities (**Supplemental Figure S6**); galactomannan binders permit the SiNPs to reach steady capacities of ~2000 mAh g^{-1}.

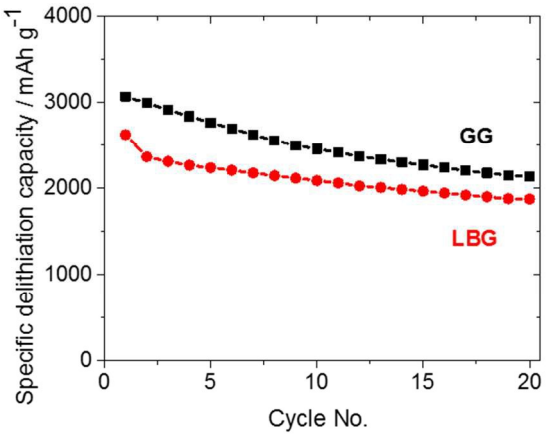

Figure 5. The delithiation capacities of SiNP/GG and SiNP/LBG electrodes using a symmetric charge/discharge rate of 0.05-C and electrode composition of 85:10:5, SiNPs:C:Binder wt%.

Electrodes using galactomannans as the binding agent retain a large amount of the initial lithiation capacity under deep-lithiation conditions (1 V to 10 mV vs Li/Li^+). On the formation cycle, a single cycle at 0.05-C (180 mA g^{-1}), typical lithiation capacities > 3600 mAh g^{-1} and coulombic efficiencies exceeding 85% are observed in SiNP/galactomannan electrodes (**Supplemental Figure S7**). While such high coulombic efficiencies were observed in SiNP/CMC electrodes, SiNP/PVDF displayed coulombic efficiencies of ~20%. The poor performance of SiNP/PVDF electrodes has been reported elsewhere[10,33]. The irreversible capacity loss on the formation cycle is attributed to SEI formation on the large surface area electrodes (SiNPs have an as-received surface area of 70-100 m^2 g^{-1}) and the presence of Si surface oxide groups. The overpotential in the initial lithiation cycle may be attributed to the native-oxide film decelerating the already sluggish redox kinetics of SiNPs[24].

Cyclic voltammetry of the SiNP/galactomannan electrodes provides further assessment on the reduction of the native-oxide layer. The current continues to increase after 9 cycles at a slow scan rate (0.2 mV s^{-1}) as more SiO_x reduces to active Si^0 and becomes available for lithiation (**Figure 6**). An increase in current

with cycle number may also be attributed to crystalline Si morphing into the amorphous phase. A stable current is typically achieved after thirteen cycles (**Supplemental Figure S8**). The CVs of the SiNP/GG electrodes also provide evidence suggesting why GG performs better than LBG as a binder in a Li-ion half-cell. The reason stems from a difference in conjugate redox peaks, where lithiation/extraction peaks in SiNP/GG electrodes are observed in a smaller potential range than the redox peak of SiNP/LBG electrodes. The voltammogram of SiNP/GG electrodes exhibits a cathodic peak (i) related to high-voltage lithiation at 190 mV and the conjugate anodic peak (iii) at 525 mV. The difference in voltage between the pair is 335 mV. SiNP/LBG electrodes display a larger separation of 360 mV between peaks (i) and (iii). Furthermore, an additional peak (ii) in the anodic polarization of SiNP/GG electrodes relating to a low-voltage delithiation was not distinctly observed in SiNP/LBG electrodes. The results suggest either slower kinetics or greater irreversibility of lithiation/extraction in the SiNP/LBG electrodes.

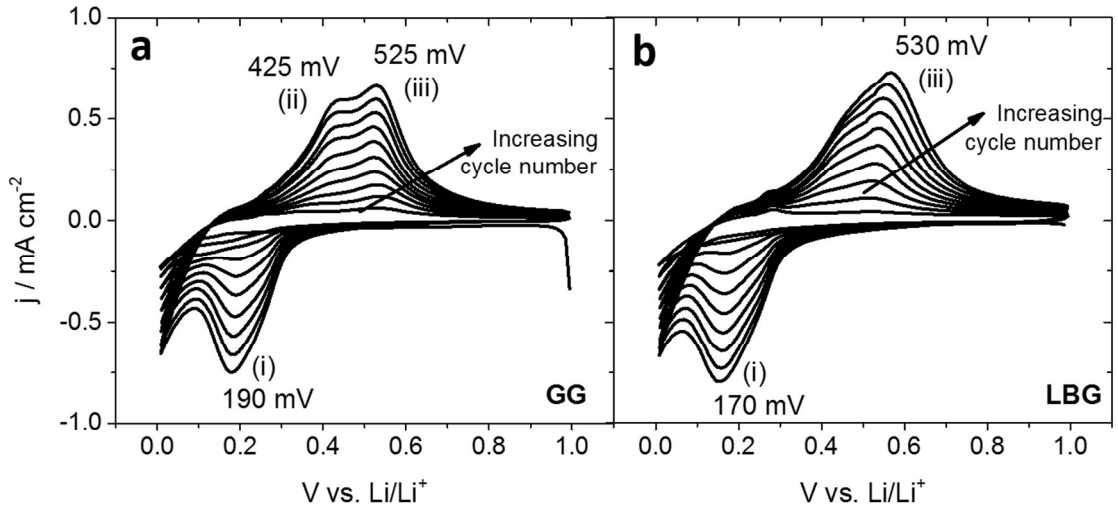

Figure 6. Cyclic voltammograms of (a) SiNP/GG and (b) SiNP/LBG electrodes. The half-cells were scanned between 1 V and 0.01 V vs Li/Li^+ using a scan rate of 0.2 mV s^{-1}. Electrode composition is 85:10:5, SiNPs:C:Binder wt%.

The SiNP electrodes were subject to 250 symmetric charge/discharge cycles at 1-C (3.6 A g^{-1}) to provide insight on the cycling life of galactomannan binders (**Figure 7a**). All electrodes with biopolymer binders exhibit ~90% capacity retention over the first 100 cycles as sufficient polymer-SiNP interactions in the biopolymers allow for electrode stability. The PVDF binder does not hydrogen bond to the SiNP oxide

surface, but rather forms weak van der Waals interactions resulting in poor LIB performance. The PVDF binder cannot withstand the large volume expansion of lithiation, and the electronically resistive SEI forms between SiNPs leading to premature cell failure. After 100 cycles, SiNP/GG, LBG, and CMC electrodes retain delithiation capacities of 1000, 860, and 700 mAh g^{-1}, respectively. It should be noted that the SiNP electrodes using biopolymer binders exhibited stable discharge capacities over the initial 100 cycles in the absence of fluoroethylene carbonate (FEC), an electrolyte additive known to enhance the stability and cycling life of Si-based electrodes[34]. While the capacities begin to fade after 100 cycles, coulombic efficiencies remain ~99% indicating a highly reversible system with the formation of a stable SEI.

Electrodes using GG as a binding agent also outperform SiNP/CMC electrodes in symmetric charge/discharge rate capability studies (**Figure 7b**). SiNP/GG electrodes exhibit capacities of 1900 mAh g^{-1} at a 0.5-C rate (1.8 A g^{-1}). The larger extent of swelling coupled with the preservation of the pre-cycled SiNP microstructure apparently allows for enhanced Li transport and electronic contact in SiNP/GG electrodes when compared to SiNP/CMC electrodes. Interestingly, SiNP/LBG electrodes perform poorly at 2-C rates. An understanding of the phenomenon is under further investigation, however, we speculate the low capacity stems from self-association of the mannan-rich regions; more mannose-mannose interactions decreases the amount of free galactose sites that can form favorable interactions with the SiNP native-oxide layer, which yields large areas of insoluble/unswelled polymer.

In addition to the high capacity observed in SiNP/GG electrodes, the GG binder also permits fast Li-extraction for high-rate performances (**Figure 7c**). The initial cycle, identical to a conditioning cycle, allows for large amounts of lithium insertion. Although not typical, SiNP electrodes exhibited lithiation capacities > 3.6 Ah g^{-1}—the capacity of $Li_{3.75}Si$ and proposed maximum capacity of silicon at ambient temperatures. The additional capacity beyond 3.6 Ah g^{--1} may be attributed to electrolyte reduction (> 200 mAh g^{-1}) and the formation of $Li_2Si_2O_5$ and Li_4SiO_4 from SiO_x reduction[24]. The reduction of SiO_x is a kinetically slow reaction and is one reason for an overpotential on the first lithiation cycle. After lithiation

at 0.05-C, SiNP/GG electrodes outperform SiNP/CMC electrodes and exhibit delithiation capacities of 3368, 3049, 2875, and 2311 mAh g^{-1} at 0.25-C, 1-C, 2-C, and 5-C, respectively. The discharge capacity observed at 5-C (18 A g^{-1}) amounts to a 68% capacity retention when compared to the initial delithiation at 0.05-C. Similar to a CV, differential delithiation-capacity curves (**Supplemental Figure S9**) provide Li-extraction potentials, which offer insight into the kinetics of the Li-extraction process. A peak potential increase of 80 mV is observed in high-potential Li_xSi phase delithiation when current increased from 0.05-C to 1-C. When the delithiation rate increases by two orders of magnitude, from 0.05-C to 5-C, a 180 mV peak potential increase is observed. To compare, SiNP/CMC electrodes exhibit a 280 mV increase in delithiation peak potential when current density increases from 0.05-C to 5-C. The high-discharge capacities and low potential at which Li-extraction occurs in SiNP/GG electrodes may lead to a more energy dense anode. High Li-extraction capacities stem from thinness of the GG coating at low-binder concentrations in the electrodes, which undergoes less mechanical stress during expansion and facilitates the transfer of Li-ions through the binding material. The low-binder content also allows for excellent capacity retention, with a delithiation capacity of 3405 mAh g-^{1} during a subsequent 0.05-C cycle (**Supplemental Figure S9**). Similarly, high-delithiation capacities are observed in SiNP/LBG electrodes.

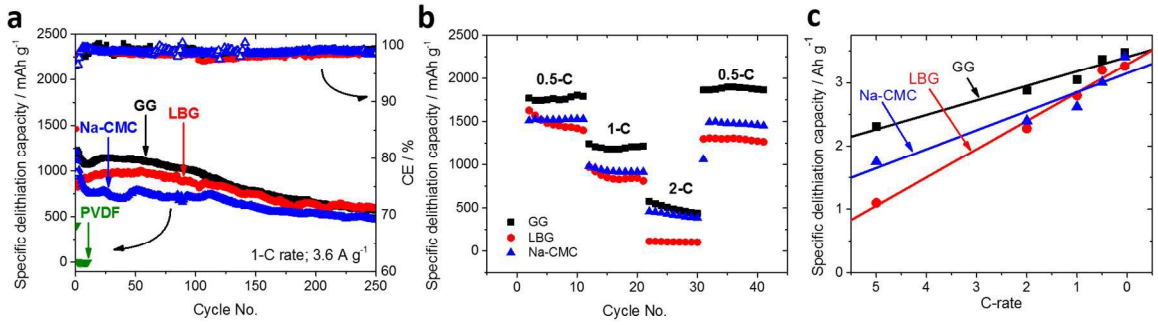

Figure 7. a) The symmetrical cycling performance of SiNPs with GG, LBG, Na-CMC and PVDF binders. After 250 cycles at 3.6 A g^{-1}, both SiNP/LBG and GG show superior capacity to SiNP/CMC and PVDF. The columbic efficiency (CE) of all SiNP electrodes using biopolymer binders remains >99% throughout cycling; b) Rate capability of the SiNPs electrodes using biopolymer binders at symmetric 0.5, 1 and 2-C rates; c) Delithiation capacities of SiNP electrodes from asymmetric charge-discharge using various binders. All Li-insertion was performed at 0.05-C to ensure full electrode lithiation while Li-extraction was performed at an increasing C-rate. The GG binder is capable of allowing Li to extract at high rates, i.e. 2300 mAh g^{-1} at 18 A g^{-1}. Electrode composition is 85:10:5, SiNPs:C:Binder wt%.

Capacities further increase in SiNP/GG electrodes when the binder content rises from 5 to 15 wt% (**Figure 8**), with these electrodes still outperforming SiNP/CMC electrodes. For example, symmetrical 0.5-C charge/discharge rates of SiNP electrodes with 15 wt% GG result in a capacity of 2500 mAh g^{-1} as compared with a 1750 mAh g^{-1} capacity in SiNP electrodes with 5 wt% GG content. Typical values for initial capacity upon half-cell conditioning further increased with binder loading while maintaining high coulombic efficiencies of ~88% (**Supplemental Figures S7 and S10**). The larger galactomannan concentration provides more electrolyte in the electrode, increasing the capacity at higher charge/discharge rates. However, capacity retention in all 15 wt% biopolymer binders began to fade after ~40 cycles. The origin of the capacity fade is under further investigation, but we speculate the increased thickness of the binder film encapsulating the SiNPs may not cope with the large mechanical stresses during lithiation. While capacity retention may be improved by electrolyte additives such as FEC, these studies are beyond the scope of the current work. Again, we see the capacity fade in SiNP electrodes using 15 wt% binder upon prolonged cycling (**Supplemental Figure S11**); after 100 cycles at 1-C (3.6 A g^{-1}), SiNPs with 15 wt% GG retain only 47% of their original capacity compared to an 80% capacity

retention observed in electrodes using 5 wt% GG. Unlike the galactomannan binders, SiNP/CMC electrodes experience no further improvements in rate capability when binder content increased from 5 to 15 wt%. The unchanged capacity when Na-CMC content is increased may originate from the particle-binder interactions; the highly polar carboxyl groups of Na-CMC provides a stronger H-bond with SiNPs than does the hydroxyl moiety with galactomannans.

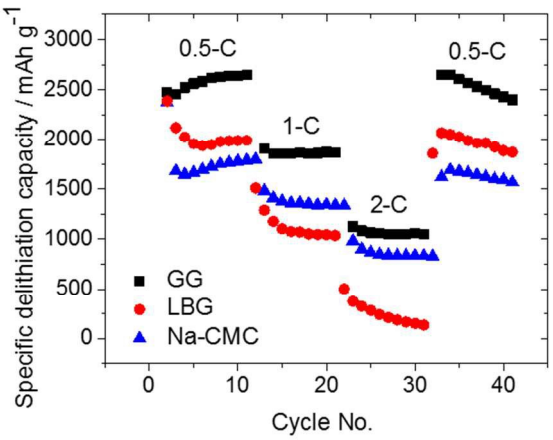

Figure 8: Rate performance for biopolymer binders reveal that SiNP/GG elctrodes are capable of the highest capacities while SiNP/LBG electrodes suffer large capacity losses at elevated currents. Electrodes composition is 75:10:15, SiNP:C:binder.

The role of any binder is to 1) protect the active material from mechanical and chemical degradations while 2) maintaining a homogenous mixture of components and 3) permitting the passage of Li-ions and electrons through the binding matrix. The > 90% capacity retention after 100 cycles and the undisrupted nano/ microstructure of the SiNPs after cycling are evidence that galactomannans may be used as a binder for SiNP electrodes. A common thread among many Si binding agents, be it glucose derivatives such as alginate, Na-CMC, and galactomannans or polymers such as polyacrylic acid, is that they are all thickening agents that utilize H-bonding to both increase the viscosity of an aqueous solution and interact with the surface oxide layer of SiNPs. High capacities and good rate capabilities have been attributed to such interactions[35]. However, one key difference is the functional group present in the H-bonding mechanism. PAA, Na-CMC, and alginate are all polyelectrolytes that bind through the stronger, more polar carboxyl moiety. The polyelectrolytic nature of the polymers may also influence Si interactions.

Galactomannans are neither charged nor have carboxyl moieties, suggesting that the polarity of hydroxyl groups is sufficient for Si-particle binding and mechanical strength during lithiation.

Conclusions

The main goal of this study was to integrate novel and environmentally friendly binder components into lithium-ion batteries with an emphasis on low-cost materials that allow Si-based electrodes to operate with high energy densities. We successfully showed that galactomannans, more specifically guar gum, may be used as a binding agent for SiNP electrodes at low loadings and outperform SiNP electrodes using Na-CMC binders. The interactions between the native-oxide layer of SiNPs and the polar hydroxyl groups (more specifically the galactose side chains) inherent to galactomannans provide for excellent cyclability and capacity retention in Li-ion half-cells. Capacity retention in SiNP/GG electrodes may be attributed to the mechanical integrity of galactomannans; electrode microstructure and porosity are retained even after deep lithiation cycles. The superior electrolyte uptake capabilities of galactomannans when compared to Na-CMC correlates to lower ionic resistances, which allows for enhanced-rate performances. Due to the electrochemical stability of these biopolymers, the use of galactomannans may also be extended beyond Si-based electrodes to other anode or cathode materials.

Acknowledgements
The authors gratefully acknowledge the U.S. Department of Energy for partial support to this work and the Department of Education's GAANN fellowship for stipend support to MKD. Thanks are also due to Kimberly Dennis for assistance with rheometry and half-cell assembly, and to Prof. Jan Genzer for use of FT-IR.

Notes and References
Electronic Supplementary Information (ESI) available: ESI contains solution rheology of polymers, further information on the silicon used for the study, SEM images of SiNP electrodes using GG, LBG, Na-CMC, and PVDF binders before and after cycling, CVs of polymer-only films, change/discharge profiles of SiNPs using biopolymer binders, and the cycling data of SiNP/GG and SiNP/LBG electrodes using a higher binding content.

1. C.-X. Zu and H. Li, *Energy Environ. Sci*., 2011, **4**, 2614.

2. R. Van Noorden, *Nature*, 2014, **507**, 26.

3. J.R. Szczech and S. Jin, *Energy Environ. Sci*., 2011, **4**, 56.

4. U. Kasavajjula, C. Wang, A. J. Appleby, *J. Power Sources*, 2007, **163**, 1003.

5. H. Wu and Y. Cui, *Nano Today*, 2012, **7**, 414.

6. A. Magasinski, P. Dixon, B. Hertzberg, A. Kvit, J. Ayala, G. Yushin, *Nat. Mater*., 2010, **9**, 353.

7. H. Lin, W. Weng, J. Ren, L. Qiu, Z. Zhang, P. Chen, X. Chen, J. Deng, Y. Wang, H. Peng, *Adv. Mater*., 2014, **26**, 1217.

8. H. Wu, G. Zheng, N. Liu, T. J. Carney, Y. Yang, Y. Cui, *Nano Lett*., 2012, **12**, 904.

9. M. Wu, X. Xiao, N. Vukmirovic, S. Xun, P. K. Das, X. Song, P. Olalde-Velasco, D. Wang, A. Z. Weber, L.-W. Wang, V. S. Battaglia, W. Yang, G. Liu, *J. Am. Chem. Soc*., 2013, **135**, 12048.

10. B. Koo, H. Kim, Y. Cho, K. T. Lee, N.-S. Choi, J. Cho, *Angew. Chem*., 2012, **51**, 8762.

11. I. Kovalenko, B. Zdyrko, A. Magasinski, B. Hertzberg, Z. Milicev, R. Burtovyy, I. Luzinov, G. Yushin, *Science*, 2011, **334**, 75.

12. C. Erk, T. Brezesinski, H. Sommer, R. Schneider, J. Janek, *ACS Appl. Mater. Interfaces*, 2013, **5**, 7299.

13. M. Murase, N. Yabuuchi, Z.-J. Han, J.-Y. Son, Y.-T. Cui, H. Oji, S. Komaba, *ChemSusChem,* 2012, **5**, 2307.

14. S. Mahammad, R. K. Prud'homme, G. W. Roberts, S. A. Khan, *Biomacromolecules*, 2006, **7**, 2583.

15. V. B. Pai and S. A. Khan, *Carbohydr Polym*, 2002, **49**, 207.

16. A. Tayal, V. B. Pai, S. A. Khan, *Macromolecules*, 1999, **32**, 5567.

17. I. C. M. Dea, E. R. Morris, D. A. Rees, J. Welsh, H. A. Barnes, J. Price, *Carbohydr. Polym*., 1977, **57**, 249.

18. M. A. Cerqueira, B. W.S. Souza, J. Simões, J. A. Teixeira, M. R. M. Domingues, M. A. Coimbra, A. A. Vicente, *Carbohydr. Polym*., 2011, **83**, 179.

19. Y. Wu, W. Li, W. Cui, N. a. M, Eskin, H. D. Goff, *Food Hydrocoll*., 2012, **26**, 359.

20. B.-R. Lee, S. Kim, E.-S. Oh, *J. Electrochem. Soc*., 2014, **161**, A2128.

21. Y. K. Jeong, T. Kwon, I. Lee, T.-S. Kim, A. Coskun, J. W. Choi, *Energy Environ. Sci*., 2015, DOI**:** 10.1039/C5EE00239G.

22. N. S. Hochgatterer, M. R. Schweiger, S. Koller, P. R. Raimann, T. Wöhrle, C. Wurm, M. Winter, Electrochem. *Solid-State Lett*., 2008, **11**, A76.

23. Z.-J. Han, N. Yabuuchi, K. Shimomura, M. Murase, H. Yui, S. Komaba, *Energy Environ. Sci*., 2012, **5**, 9014.

24. S. Xun, X. Song, L. Wang, M. E. Grass, Z. Liu, V. S. Battaglia, G. Liu, *J. Electrochem. Soc*., 2011, **158**, A1260.

25. D. C. Marra, E. Z. Edelberg, R. L. Naone, E. S. Aydil, *J. Vac. Sci. Technol. A*, 1998, **16**, 3199.

26. R. O. Mannion, C. D. Melia, B. Launay, G. Cuvelier, S. E. Hill, S. E. Harding, J. R. Mitchelp, *Carbohydr. Polym*., 1992, **19**, 91.

27. M. D. Burke, J. O. Park, M. Srinivasarao, S. A. Khan, *Journal of controlled release*, 2005, **104**, 141.

28. K.S Mikkonen, H. Rita, H. Hele, R. A. Talja, L. Hyvo, *Biomacromolecules*, 2007, **8**, 3198.

29. D. R. Picout, S. B. Ross-Murphy, K. Jumel, and S. E. Harding, *Biomacromolecules*, 2002, **3**, 761.

30. Y.-M. Lin, K. C. Klavetter, P. R. Abel, N. C. Davy, J. L. Snider, A. Heller, C. B. Mullins, *Chem. Commun*., 2012, **48**, 7268.

31. J. Li, A. K. Dozier, Y. Li, F. Yang, Y.-T. Cheng, *J. Electrochem. Soc*., 2011, **158**, A689.

32. M. N. Obrovac, and L. J. Krause, *J. Electrochem. Soc*., 2007, **154**, A103.

33. G. Liu, S. Xun, N. Vukmirovic, X. Song, P. Olalde-Velasco, H. Zheng, V. S. Battaglia, L. Wang, W. Yang, *Adv. Mater*., 2011, **23**, 4679.

34. V. Etacheri, O. Haik, Y. Go, G. A. Roberts, I. C. Stefan, R. Fasching, D. Aurbach, *Langmuir*, 2012, **28**, 965.

35. M.-H. Ryou, J. Kim, I. Lee, S. Kim, Y. K. Jeong, S. Hong, J. H. Ryu, T.-S. Kim, J.-K. Park, H. Lee, J. W. Choi, *Adv. Mater*. 2013, **25**, 1571.

Graphical abstract

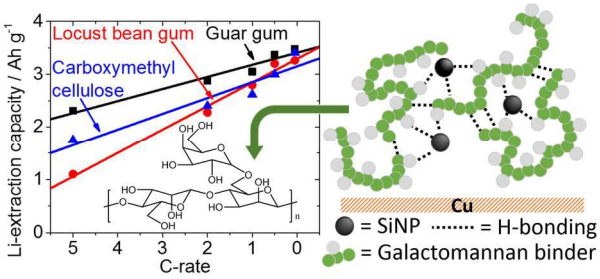

The high Li-extraction capacity can be owed to the favorable interactions between silicon nanoparticles and the galactomannan binders.